backing sheet (in comparison with the reference configuration). Estimates based on transonic similarity rules[16] show that the drag due to the increased airfoil thickness is in the range of 0.5–1% of the total drag depending on M_∞ and α. The drag due to the step on the top and bottom surfaces, estimated using the correlation given by Gaudet and Winter,[17] is about 1% of the total drag for the conditions of the test. These corrections, if taken into account, would result in skin-friction drag reduction better than the 6–12% indicated.

Figure 4 displays wake pitot profiles, with and without the riblet, for two flow conditions (where P_y is the pitot pressure in the wake). The results show that a larger contribution to the drag reduction results from the airfoil upper surface with increase in adverse pressure gradients.

Conclusions

Experiments have been made to assess viscous drag reduction using 3M riblets on a supercritical airfoil at transonic speeds. The airfoil angle of attack was varied between −0.5 to 1 deg. Results show skin-friction drag reduction in the range of 6–12% for the conditions of the test, which is higher than what has been observed in zero pressure gradient flows. These results suggest increased effectiveness of riblets in adverse pressure gradients.

Acknowledgment

This work was carried out under a grant received from the Aeronautical Development Agency, Bangalore, India.

References

[1]Walsh, M. J., "Riblets," *Viscous Drag Reduction in Boundary Layers*, Vol. 123, Progress in Astronautics and Aeronautics, AIAA, Washington, DC, 1990, pp. 203–261.

[2]Coustols, E., "Control of Turbulence by Internal and External Manipulators," 4th International Conference on Drag Reduction, Davos, Switzerland, July–Aug. 1989.

[3]Wilkinson, S. P., Anders, J. B., Lazos, B. S., and Bushnell, D. M., "Turbulent Drag Reduction Research at NASA Langley: Progress and Plans," Proc., *Turbulent Boundary Layer Drag Reduction by Passive Means*, Royal Aeronautical Society, London, 1987, pp. 1–32.

[4]Sundaram, S., and Viswanath, P. R., "Study on Turbulent Drag Reduction Using Riblets on a Flat Plate," National Aerospace Lab., NAL PD EA 9209, Bangalore, India, Nov. 1992.

[5]McLean, J. D., George-Falvy, D. N., and Sullivan, P. P., "Flight-Test of Turbulent Skin-Friction Reduction by Riblets," *Proc., Turbulent Boundary Layer Drag Reduction by Passive Means*, Royal Aeronautical Society, London, 1987, pp. 408–424.

[6]Walsh, M. J., and Sellers, W. L., "Riblet Drag Reduction at Flight Conditions," AIAA Paper 88-2554, June 1988.

[7]Squire, L. C., and Savill, A. M., "Some Experiences of Riblets at Transonic Speeds," *Proc., Turbulent Boundary Layer Drag Reduction by Passive Means*, Royal Aeronautical Society, London, 1987, pp. 392–407.

[8]Coustols, E., and Schmitt, V., "Synthesis of Experimental Riblet Studies in Transonic Conditions," *Turbulence Control by Passive Means*, edited by E. Coustols, Kluwer, Dordrecht, The Netherlands, 1990, pp. 123–140.

[9]Viswanath, P. R., and Mukund, R., "Aerodynamic Characteristics of a Laminar Supercritical Aerofoil at Transonic Speeds," National Aerospace Lab., NAL PD EA 9311, Bangalore, India, Nov. 1993.

[10]Kacprzynski, J. J., Ohman, L. H., Garabedian, P. R., and Korn, D. G., "Analysis of the Flow Past a Shockless Lifting Airfoil in Design and Off-Design Conditions," National Research Council (Canada), Aeronautical Report LR-544, Ottawa, Nov. 1971.

[11]Desai, S. S., Parikh, P. C., and Ramaswamy, M. A., "On an Approximate Formula for the Evaluation of Drag from Wake Survey Measurements," National Aerospace Lab., NAL Rept. AE-TM-2-79, Bangalore, India, July 1979.

[12]Kline, S. J., and McClintock, F. A., "Describing Uncertainties in Single-Sample Experiments," *Mech. Eng.*, Jan. 1953, pp. 3–8.

[13]Desai, S. S., and Kiske, S., "A Computer Program to Calculate Turbulent Boundary Layer and Wakes in Compressible Flow with Arbitrary Pressure Gradient Based on Greens Lag-Entrainment Method," Inst. of Thermofluid Dynamic, Ruhr Univ., Bericht No. 89/1982, Bochum, Germany, Jan. 1982.

[14]Sundaram, S., and Viswanath, P. R., "Studies of Turbulent Drag Reduction Using Riblets on a NACA 0012 Aerofoil," National Aerospace Lab., NAL PD EA 9401, Bangalore, India, Jan. 1994.

[15]Nieuwstadt, F. T. M., Wolthers, W., Leijdens, H., Krishna Prasad, K., and Schwarz-van Manen, A., "The Reduction of Skin Friction by Riblets Under the Influence of an Adverse Pressure Gradient," *Experiments in Fluids*, Vol. 15, No. 1, 1993, pp. 17–26.

[16]Spreiter, J. R., "On the Application of Transonic Similarity Rules to Wings of Finite Span," NACA Rept. 1153, 1953.

[17]Gaudet, L., and Winter, K. G., "Measurements of the Drag of Some Characteristic Aircraft Excrescences Immersed in Turbulent Boundary Layers," Royal Aircraft Establishment, Aerodynamics Drag, AGARD CP-124, Farnborough, England, UK, Oct. 1973, pp. 4.1–4.12.

Sensitivity of Amplification-Factor Transition Criterion for Flow over Roughness Element

Jamal A. Masad*

High Technology Corporation,
Hampton, Virginia 23666

LINEAR stability theory coupled with the empirical e^N method[1,2] is a common approach that is widely used to predict transition location in engineering applications. In this approach, the integrated growth rate (N factor) calculated using linear stability theory is correlated with the onset of laminar turbulent transition. It was found[1–4] that the location at which the value of N is in the range from 9 to 11 correlates well with the transition onset location in two-dimensional flows. The predictions of the approach showed good agreement with transition experimental data obtained in a low-disturbance environment such as quiet wind tunnels[3] and under flight conditions.[4] In the case of flow over roughness elements, the predictions of the e^N method agreed reasonably well even with relatively noisy wind-tunnel transition data.[5,6] Bushnell and Reshotko[7] pointed out that "at supersonic speeds, roughness is such an overriding transition bypass that the research can be conducted in conventional, noisy, tunnels."

The dependence of the predicted transition onset location on the value of N can be quantified by considering the sensitivity of the e^N method. The sensitivity of the e^N method is denoted by σ_N and defined as the rate of change of correlated transition Reynolds number $(Re_x)_N$ with respect to N divided by the correlated transition Reynolds number. Therefore,

$$\sigma_N = \frac{1}{(Re_x)_N}\frac{\mathrm{d}(Re_x)_N}{\mathrm{d}N} \tag{1}$$

where

$$Re_x = U_\infty^* x^* / \nu_\infty^* \tag{2}$$

and U_∞^* is the dimensional freestream streamwise velocity, ν_∞^* is the dimensional freestream kinematic viscosity, and x^* is the dimensional distance measured from the leading edge. The value $(Re_x)_N$ is the smallest Reynolds number value (sweeping over all frequencies) at which the N factor reaches the value N. For example, in incompressible flow over a smooth flat plate and using $N = 9$, the value of σ_N is 0.168. This implies that the predicted value of $(Re_x)_N$ will vary by about ±16.8% if the correlating N factor was chosen to be 10 or 8 instead of 9. In this work, we evaluate the sensitivity σ_N for the case of flow over a roughness element that might cause the flow to separate.

We consider a two-dimensional incompressible flow around a single smooth two-dimensional hump on a flat plate. We consider a two-parameter family of symmetric hump shapes given by

$$y = y^*/L^* = (h^*/L^*) f(z) = h f(z) \tag{3}$$

Received May 27, 1994; revision received Sept. 23, 1994; accepted for publication Sept. 30, 1994. Copyright © 1994 by the American Institute of Aeronautics and Astronautics, Inc. All rights reserved.

*Research Scientist. Senior Member AIAA.

where

$$z = 2(x^* - L^*)/\lambda^* = 2(x-1)/\lambda \tag{4}$$

and

$$f(z) = \begin{cases} 1 - 3z^2 + 2|z|^3, & \text{if } |z| \le 1 \\ 0, & \text{if } |z| > 1 \end{cases} \tag{5}$$

Here h^* is the symmetric hump dimensional height, and λ^* is the dimensional length of the hump with the center located at $x^* = L^*$.

The roughness element under consideration could produce a separation bubble behind it. In such flows, both a strong viscous-inviscid interaction and an upstream influence exist. The conventional boundary-layer formulation fails to predict such flows; therefore, we use the interacting boundary-layer (IBL) theory (see Nayfeh et al.[5]) to analyze them.

Following the computation of the mean flow using the IBL theory, linear quasiparallel stability analysis is performed on the resulting velocity profiles. Only two-dimensional disturbances are considered because these are the most amplified in the incompressible two-dimensional flow under consideration. The frequency of the disturbance F is defined as

$$F = 2\pi f^* \nu_\infty^* / U_\infty^{*2} \tag{6}$$

where f^* is the dimensional frequency in cycles per second (Hz). The frequency F remains fixed for the same physical wave as it is convected downstream.

Variation of predicted transition Reynolds number with $N = 8, 9,$ and 10 with the nondimensional height of the roughness h is shown in Fig. 1. The nondimensional length of the roughness is $\lambda = 0.2$ and the freestream Reynolds number based on the distance from the leading edge to the center of the hump is $Re = 0.8 \times 10^6$. The filled circles indicate that the flow separates and reattaches, and the hollow circles indicate that the flow remains attached. The values of h considered extend between $h = 0.0002$ and 0.0042 in steps of 0.0002. The predicted transition Reynolds numbers in Fig. 1 decrease gradually as h is increased, then they decrease sharply and finally saturate to an almost constant value which is independent even of the value of N used to correlate transition. The variation of the sensitivity to the value of 9 with h for the results shown in Fig. 1 is shown in Fig. 2. It is clear from Fig. 2 that once the flow separates, the sensitivity starts increasing considerably, reaches a maximum, and then drops very sharply to a value slightly larger than zero. At $h = 0.0002$ the sensitivity σ_9 is 0.158. The maximum σ_9, 0.389, is at $h = 0.0028$, and the minimum σ_9, 0.012, is at $h = 0.0042$. This means that at $h = 0.0028$ the predicted value of $(Re_x)_N$ will vary by about $\pm 38.9\%$ if the correlating N factor was chosen to be 10 or 8 instead of 9. Similarly, at $h = 0.0042$, the predicted value of $(Re_x)_N$ will vary only by $\pm 1.2\%$ if the correlating N factor was chosen to be 10 or 8 instead of 9. The reason for the large sensitivity between when the flow separates and until the transition location saturates is that at the lowest height causing saturation all the strong growth in the separation bubble is used to just reach a desired N value. Reducing the height beyond that point requires additional contribution from the small growth rates in the almost recovered Blasius flow downstream of the roughness in order for N to reach the desired value. This results in a large value of $(Re_x)_{N=10}$ which gets reflected in the sensitivity.

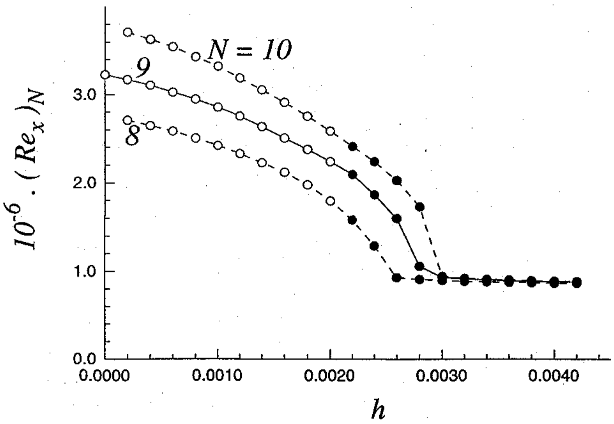

Fig. 1 Variation of predicted transition Reynolds number with the roughness height at $\lambda = 0.2$ and $Re = 0.8 \times 10^6$.

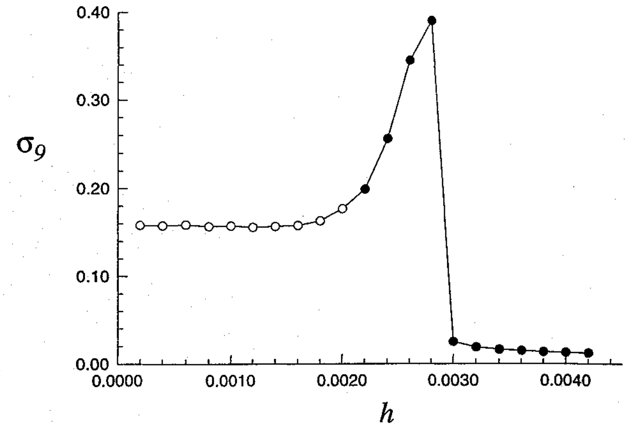

Fig. 2 Variation of the sensitivity σ_9 with h for the conditions of Fig. 1.

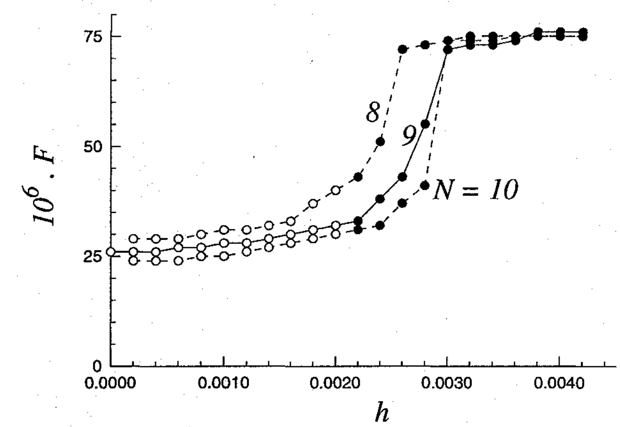

Fig. 3 Variation of frequency predicted to cause transition with h for the conditions of Fig. 1.

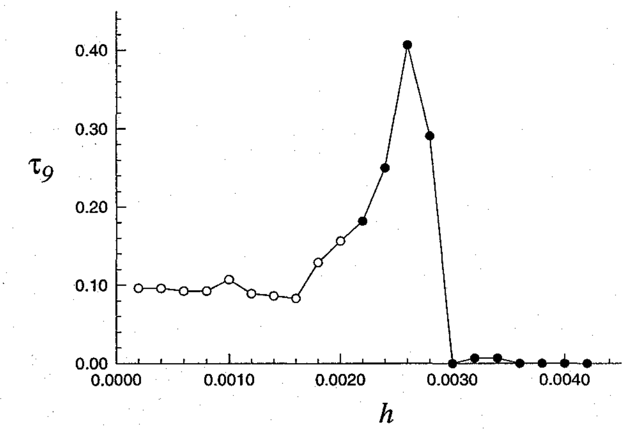

Fig. 4 Variation of the sensitivity τ_9 with h for the conditions of Figs. 1 and 3.

The variation of frequency predicted to cause transition in the results of Fig. 1 with h is shown in Fig. 3. It is clear from comparing Figs. 1 and 3 that as $(Re_x)_N$ decreases, the frequency predicted to cause transition increases. We can define the sensitivity of the frequency to the value of N as

$$\tau_N = -\frac{1}{F}\frac{\mathrm{d}F}{\mathrm{d}N} \tag{7}$$

The variation of τ_9 with h for the results of Fig. 3 is shown in

Fig. 4. It is clear from Fig. 4 that τ_9 follows a trend similar to the trend of the variation of σ_9.

References

[1]Smith, A. M. O., and Gamberoni, N., "Transition, Pressure Gradient and Stability Theory," Rept. ES 26388, Douglas Aircraft Co., El Segundo, CA, Aug. 1956.

[2]Jaffe, N. A., Okamura, T. T., Smith, A. M. O., "Determination of Spatial Amplification Factors and their Application to Predicting Transition," *AIAA Journal*, Vol. 8, 1970, pp. 301–308.

[3]Malik, M. R., "Prediction and Control of Transition in Supersonic and Hypersonic Boundary Layers," *AIAA Journal*, Vol. 27, No. 11, 1989, pp. 1487–1493.

[4]Masad, J. A., and Malik, M. R., "Comparison of Linear Stability Results with Flight Transition Data," *AIAA Journal*, Vol. 33, No. 1, 1995, pp. 161–163.

[5]Nayfeh, A. H., Ragab, S. A., and Al-Maaitah, A. A., "Effect of Bulges on the Stability of Boundary Layers," *Physics of Fluids*, Vol. 31, No. 4, 1988, pp. 796–806.

[6]Masad. J. A., and Iyer, V., "Transition Prediction and Control in Subsonic Flow Over a Hump," *Physics of Fluids*, Vol. 6, No. 1, 1994, pp. 313–327; also NASA CR-4543, Sept. 1993.

[7]Bushnell, D. M., and Reshotko, E., "Status of NASP Boundary-Layer Transition Research: Summary of the 3rd NASP Transition Workshop," NASP Workshop Pub. 1006, Jan. 1990.

Two-Dimensional Shear-Layer Entrainment and Interface-Length Measurements

Tzong H. Chen*
Systems Research Laboratories, Inc., Dayton, Ohio 45440
and
Robert D. Hancock†
Wright Laboratory, Wright–Patterson Air Force Base, Ohio 45433

Introduction

LARGE-SCALE vortices have been studied extensively for many years. The development of these vortices is viewed as a key mechanism in the promotion of macroscale mixing that creates the environment in which microscale mixing can induce chemical reactions. In the present study, a novel approach was utilized to investigate the effect of vortex roll-up on entrainment, interface length, and mixing. The unique interface-tracing technique developed and demonstrated in this investigation allows direct study of the mixing and reaction along the interface. Entrainment of fluids from both sides of the mixing layer was measured after locating the interface boundary. Thus, the mixing and reaction enhancement can be directly compared with the measured interface elongation for the first time. This allows direct evaluation of the efficiency of mixing enhancement by increasing the interface length through vortex roll-up.

This Note will provide a brief description of the experimental setup. (Details can be found in the original full length paper.[1]) Two-dimensional vortices are generated from a splitter plate that separates two parallel streams of air, one high speed, one low, contained within a 12.7-cm-square Plexiglas duct. The splitter plate divides the duct into two equal areas. Dry air is used on both sides. A technique known as reactive Mie scattering[2] is used to visualize the vortical flow. Air on the high-speed side of the splitter plate is passed over a liquid $TiCl_4$ bath, collecting $TiCl_4$ vapor. Air on the low-speed side of the splitter plate is passed over a water bath, collecting water vapor. The $TiCl_4$ in the higher velocity airflow reacts with the moist air on the low-velocity side of the flow, forming micron-sized TiO_2 particles that follow the gas flow and distinctly mark the molecular interface of the two airstreams. The velocity of the air on the high-velocity (left) side of the flow was 0.94 m/s and that on the low-velocity (right) side was 0.47 m/s. Vortex formation and shedding are driven by acoustic stimulation of the low-speed flow, which can be controlled with great consistency, which is essential for phase-locked measurements. Some data were obtained in undriven shear layers with additional measurements being made in identical flows driven at 15, 20, and 25 Hz. The flowfield is recorded as a digital image on a portion of a 1024 × 1024 diode array. Typically, the image size was 250 × 1024 pixels, with the 1024 pixels oriented parallel to the flow direction. The light source is the frequency-doubled output (532 nm) of an Nd:YAG laser. The image is collected with a charge-coupled device (CCD) camera and analyzed in its original form.

Results and Discussions

Figure 1 shows, at six different phase angles, a two-dimensional shear layer being driven at 20 Hz. These images were obtained by increasing the delay time between the generation of the vortex and the CCD camera exposure. The excellent repeatability of the driven flow makes phase-locked measurements possible.

A computer algorithm was developed for tracing two lines of constant intensity on the shear layer in the digitized images. These constant-intensity contour lines are illustrated in Fig. 2. These two lines mark interface surfaces for the fluid on the left and right sides of the flow with the TiO_2 product. The area between the two lines thus represents the mixed region, or the region where the TiO_2 product resides. The phase-locking capability allows vortices to be followed in a Lagrangian frame of reference because the flow is phase locked with the CCD camera. Since individual vortices were singled out in the flow, a method was needed for establishing a bounded region within which to measure areas and interface lengths. The method selected was to draw a box around the vortex with the top and bottom edges of the box being located halfway between adjacent vortex centers near the stagnation points. The sides of the box were drawn tangent to the extreme edges of the vortex. The area and interface lengths were then calculated with the computer algorithm developed for that purpose. From these measurements, the entrainment and resultant interface length were derived and studied parametrically as a function of driving frequency.

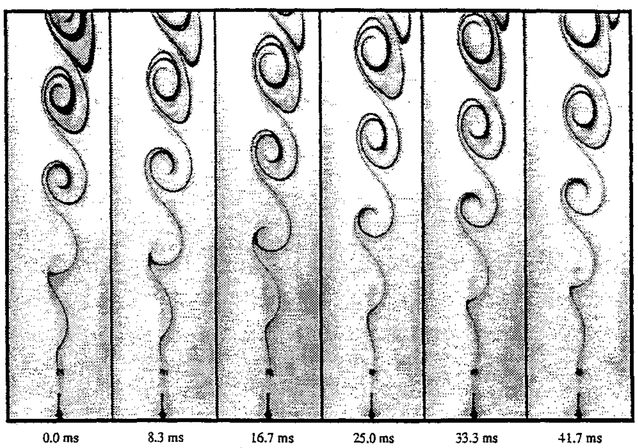

Fig. 1 Phase-locked images of a two-dimensional shear layer driven at 20 Hz.

Received May 30, 1992; presented as Paper 93-0382 at the AIAA 30th Aerospace Sciences Meeting, Reno, NV, Jan. 6–9, 1993; revision received June 16, 1994; accepted for publication June 28, 1994. Copyright © 1994 by Tzong H. Chen and Robert D. Hancock. Published by the American Institute of Aeronautics and Astronautics, Inc., with permission.

*Senior Research Scientist, Research Applications Division; currently at Taitech, Inc., 3675 Harmeling Drive, Beavercreek, OH 45440. Senior Member AIAA.

†Aero Space Engineer, Fuel and Combustion Division. Member AIAA.